Interface and chain confinement effects on the glass transition temperature of thin polymer films

J. A. Forrest,*,† K. Dalnoki-Veress, and J. R. Dutcher*
Department of Physics and Guelph-Waterloo Program for Graduate Work in Physics, University of Guelph, Guelph, Ontario, Canada N1G 2W1
(Received 15 April 1997)

We have used Brillouin light scattering and ellipsometry to measure the glass transition temperature T_g of thin polystyrene (PS) films as a function of the film thickness h for two different molecular weights M_w. Three different film geometries were studied: freely standing films, films supported on a SiO_x surface with the other film surface free (uncapped supported), and films supported on a SiO_x surface and covered with a SiO_x layer (capped supported). For freely standing films T_g is reduced dramatically from the bulk value by an amount that depends on both h and M_w. For $h \lesssim R_{EE}$ (the average end-to-end distance of the unperturbed polymer molecules), T_g decreases linearly with decreasing h with reductions as large as 60 K for both M_w values. We observe a large M_w dependence of the T_g reductions for freely standing films which provides the first strong evidence of the importance of chain confinement effects on the glass transition temperature of thin polymer films. For both the uncapped and capped supported films, T_g is reduced only slightly (<10 K) from the bulk value, with only small differences in T_g (<4 K) observed between uncapped and capped supported films of the same thickness. The results of our experiments demonstrate that the polymer-substrate interaction is the dominant effect in determining the glass transition temperature of PS films supported on SiO_x. [S1063-651X(97)00711-3]

PACS number(s): 36.20.−r, 64.70.Pf, 68.60.Bs, 78.35.+c

INTRODUCTION

Recently there has been much interest in the physical properties of thin polymer films [1,2]. As very thin films are incorporated into device applications, it is necessary to have a good understanding of their physical properties. A more detailed knowledge of polymer interfaces could also be helpful in the design of surface modification procedures with further application to such areas as biocompatibility. At a more fundamental level, the creation of polymer samples in thin-film geometry enables one to explore variables and combinations of variables not possible in the bulk; in this way one might gain a better understanding of polymers in general.

The large surface-area-to-volume ratio in the thin film geometry allows one to study interfacial effects and in particular the role of free versus supported surfaces with various physical and/or chemical affinities. The film thickness becomes an important parameter, as this can be varied on a scale comparable to the length scale set by the polymers themselves. By reducing the thickness of a film appropriately one must eventually perturb the conformation of the polymer molecules and these confinement restrictions may affect the mechanical properties of the sample. Foremost among these properties, and almost certainly the least understood, is the glass transition temperature T_g. For temperatures below T_g the polymer is hard and glassy, and for temperatures above T_g it is soft and rubberlike.

Because of the importance of understanding the glass transition in thin polymer films, there have been a large number of recent experimental studies. These experiments have consisted of both direct measurements of T_g and related measurements of chain and segmental mobility in polymer thin films, and have involved a variety of techniques ranging from ellipsometry to x-ray reflectivity with surprising and sometimes contradictory results. All of this work, with the exception of Ref. [3], has been performed on polymer films supported on substrates with the other film surface free (uncapped supported films), since these samples are relatively easy to prepare and are important for technological applications. We now summarize the results of these experiments, specifying, whenever possible, the polymer film thickness h, the polymer molecular weight M_w, and the average end-to-end distance of the unperturbed polymer molecules $R_{EE} \sim 2R_g$.

The first direct measurements of the dependence of T_g on film thickness for uncapped supported polymer films were performed by Keddie, Jones, and Cory using ellipsometry [4]. For polystyrene (PS) films prepared on hydrogen-passivated silicon (Si-H) substrates, T_g was reduced from the bulk value for film thickness values $h<400$ Å. Keddie, Jones, and Cory measured T_g for a large number of films (~ 50) with 100 Å$<h<$3000 Å for polymers with three different M_w values (PS $M_w = 120\times10^3$, 501×10^3, and 2900×10^3; $R_{EE}=225$, 460, and 1110 Å). The measured T_g values for samples of all M_w values were described collectively by the empirical relation

$$T_g(h) = T_g^{\text{bulk}}\left[1-\left(\frac{\alpha}{h}\right)^{\delta}\right]. \tag{1}$$

The best fit of the data to Eq. (1) was obtained for $\alpha = 32$ Å and $\delta = 1.8$. This quantitative agreement between the measured T_g values for polymers with M_w values differing by a factor of 25 provided strong evidence that confinement of the

*Authors to whom correspondence should be addressed.
†Present address: Department of Physics, Chalmers University of Technology, S-412 96 Göteborg, Sweden.

polymer molecules was not responsible for the reduction in the T_g values. Instead it was suggested that the reduction in the T_g value was caused by the presence of a liquidlike layer at the polymer-air interface, with the substrate having only little effect. Estimates based on the observed thermal expansivities suggested that the characteristic length scale for this layer was $\sim 80-130$ Å. Subsequent ellipsometry measurements by Keddie, Jones, and Cory of uncapped poly(methyl methacrylate) (PMMA) films ($M_w = 100\times10^3$; $R_{EE} = 220$ Å) on two different substrates revealed the dominant effect of the polymer-substrate interaction in determining the T_g values measured for uncapped supported films [5]. For PMMA films deposited onto the native oxide coating of Si wafers (150 Å$< h <$1200 Å), the measured T_g values increased with decreasing film thickness h, whereas for PMMA films deposited onto Au-coated Si wafers (300 Å$< h <$1300 Å), the measured T_g values decreased as h was reduced. It was proposed that a strongly attractive interaction between PMMA and the Si native oxide due to hydrogen bonding was responsible for the increase in T_g with decreasing film thickness. The PMMA-Au interaction is much weaker, leading to a decrease in T_g with decreasing film thickness. This qualitative difference in the thickness dependence of T_g for the two substrates revealed the strong influence of the polymer-substrate interaction on T_g.

X-ray reflectivity has also been used to measure the T_g values for seven different uncapped PS films on Si-H (PS $M_w = 233\times10^3$; $R_{EE} = 310$ Å) with film thicknesses 91 Å$\leqslant h \leqslant$1988 Å [6]. In principle, these films were very similar to those of Ref. [4]. The data for all of the samples with film thicknesses $h \geqslant 497$ Å were consistent with a single value of $T_g \sim 390$ K, which is 20 K larger than the accepted bulk value. Because of the absence of a glass transition signature in the data for the films with $h < 497$ Å the authors suggested that the T_g value for these films had increased to a value that was larger than that of the highest temperature probed in the experiment ($T = 433$ K). However, since the thermal expansivity of the melt can be seen in their data to decrease with decreasing film thickness, approaching that of the glass, it is more likely that the resolution of the x-ray reflectivity experiment was insufficient to observe a glass transition within the temperature range of the measurements for the films with $h < 497$ Å. It is important to realize that all of the data presented in Ref. [6], which shows no shift in T_g for $h > 497$ Å and no measured T_g values for $h < 497$ Å, are consistent with the results of Ref. [4].

X-ray reflectivity was also used to study uncapped poly-2-vinyl pyridine [P(2)VP; $M_w = 200\times10^3$; R_g estimated to be 120 Å] films on SiO_x [7], for which there is a strongly attractive polymer-substrate interaction. As expected, based on the results of Ref. [5], an increase in the measured T_g values was observed as the film thickness was decreased, with a T_g increase of 54 K for a film thickness of 77 Å.

Positron annihilation lifetime spectroscopy (PALS) has been used to infer that the T_g value near the PS-vacuum interface in uncapped supported PS films (PS $M_w = 260\times10^3$, $R_{EE} = 330$ Å) on Si-H was consistent with the bulk T_g value [8]. In more recent PALS measurements by the same group [9], they measured T_g values for various PS film thicknesses which were very similar to those reported in Ref. [4]. By analyzing their results in terms of a three-layer model, they found evidence a meltlike surface layer, which is contrary to the results of their original measurements [8].

There have also been many recent measurements of chain mobility in thin polymer films. The first direct observation of the dependence of chain mobility on polymer film thickness was obtained by Reiter in x-ray reflectivity studies of the dewetting of uncapped PS films on glass substrates [10]. For films with thicknesses less than $h \simeq 110$ Å, dewetting was observed at temperatures lower than that for thick films. For film thicknesses $h \lesssim 75$ Å, dewetting was observed *below* the bulk T_g value. Only slight differences in the dewetting temperature were observed for the two PS molecular weights ($M_w = 35\times10^3$ and 650×10^3; $R_{EE} = 120$ and 520 Å).

Chain mobility in uncapped PS films supported on silicon oxide was measured directly using fluorescence recovery after patterned photobleaching [11]. In these measurements, the lateral diffusion coefficient of the polymer chains ($M_w = 30\times10^3$; $R_{EE} = 120$ Å) was substantially lower than its bulk value for films with thicknesses much larger than R_{EE} ($h < 1500$ Å) [11]. The results of these measurements, which are in agreement with those of Zheng *et al.* [12], demonstrate that the chain mobility is strongly influenced by substrate effects. Higher mobility at the free surface relative to the bulk is expected [11], but has yet to be observed directly.

In room temperature atomic force microscopy measurements of 2000-Å-thick uncapped supported PS films ($1.7\times10^3 < M_w < 1800\times10^3$; 30 Å$< R_{EE} <$900 Å), for which h was much larger than R_{EE}, enhanced mobility of the polymer chains at the free surface of the films was observed for small molecular weights ($M_w < 27\times10^3$) [13]. These results show that the surface region of low M_w PS films is ''rubberlike'' at a temperature which is 70 K less than the bulk value of T_g, whereas the surface region of PS films with larger M_w values is glassy at room temperature.

Recently, it was shown that room temperature buffing of thin polymer films will orient the polymer chain side groups along the buffing direction, even for high-T_g polymers such as polyimide ($T_g > 400$ °C) [14,15]. This ability to rearrange the chains at the free surface of a polymer is evidence for the existence of a surface region of enhanced mobility. Near-edge x-ray-absorption fine structure has been used to study the relaxation of the buffed state of uncapped PS films supported on Si wafers with the native oxide layer [16]. For all films studied ($h > R_{EE}$), full relaxation of the buffed, oriented state was not observed for temperatures less than the bulk value of T_g.

To relate the results of chain mobility experiments to the glass transition, it is important to realize that chain mobility, which corresponds to the diffusion of whole polymer chains, requires much larger motions, e.g., reptation, than the segmental motion required for the glass transition to occur.

The cooperative segmental mobility (α-relaxation dynamics) has been measured directly for uncapped supported films of a random copolymer ($M_w = 59\times10^3$) of isobutyl methacrylate and Disperse Red 1 functionalized monomer using second-harmonic generation [17]. These measurements reveal a broadening in the distribution of relaxation times for films with $h < 900$ Å. However, no shift was observed in the average value of the relaxation time with decreasing film thickness for h as small as 70 Å, which implies that there is no corresponding change in T_g.

In addition to the large body of experimental work studying chain mobility and the glass transition for thin polymer films, there has also been substantial theoretical and simulation work on similar systems. Mayes [18] used a simple scaling argument to suggest that the T_g value near the free surface will be lower than the bulk value. This argument is based upon the concept of an increased density of chain ends near a free surface of a polymer melt [19], which is in agreement with the results of recent experiments [20]. The surface T_g was predicted to be an increasing function of the number of monomer units, N. The increased density of chain ends near the surface of a thin film could lead to a lower average T_g value [18], although such a transition would be expected to be broadened substantially in temperature.

There have been many computer simulations of polymer melts confined by hard walls and free surfaces (see, e.g., references contained in Ref. [21]). The simulations have considered the effect on the static and dynamic properties of the polymer chains of changing the chain length, density, wall separation, wall potential, and temperature. Several of these simulations are particularly relevant to confinement effects on T_g.

Two simulation studies [22,23] of melts confined between two hard walls explored the limit in which the wall spacing was comparable to or less than the R_{EE} value in the bulk melt. In particular, Pakula [22] calculated the static properties of a polymer melt between neutral walls for wall spacings H that were greater than and comparable to R_{EE}. The chain length was $N=80$, corresponding to $R_{EE}\sim 9$, and the wall spacing was varied from $H=40$ to 10. Realizing that the instantaneous shape of a polymer molecule can be described as ellipsoidal [24], Pakula showed that the effect of confinement was to orient the ellipsoidal molecules with the major axis parallel to the wall, such that the center-of-mass density increased near the wall.

Because of the long structural relaxation times associated with glasses, there have been relatively few simulations of either confined glassy polymer films or supercooled polymer melts. Mansfield and Theodorou [25,26] used molecular dynamics to study the static and dynamic properties of freely standing polypropylene films at a temperature lower than the experimental value of T_g. For their simulations of the chain dynamics, they used chains of length $N=26$. With their choice of segment length, this value of N corresponds to $R_{EE}=20$ Å, which is small compared with the 62 Å separation of the two polymer-vacuum interfaces, but equal to the ''unit-cell'' dimension in the plane of the film. They found that the center-of-mass mobility parallel to the walls was enhanced for chains located a distance of the order of R_{EE} from the free surfaces. This length scale was twice as large as that for which decreases in monomer density were observed. Baschnagel and Binder [21,27] used Monte Carlo techniques to examine the static and dynamic properties of a supercooled polymer melt confined between hard neutral walls. For their simulations, they used chains of length $N=10$. This corresponds to $R_{EE}=8$ Å, which is small compared with the 40 Å separation of the hard walls and the 40 Å dimension of the ''unit cell'' in the plane of the film. They found that the motion of the monomers and the chains parallel to the walls was enhanced, and that perpendicular to the walls was reduced, over a length scale which is of the order of R_{EE} for polymer molecules in the melt. This interfacial thickness, which also characterized changes in the monomer density and polymer size from their bulk values, was larger for the glass than for the melt.

Therefore, in simulations of polymers at temperatures near T_g confined by both free surfaces and hard neutral walls, it is found that the chain mobility in the surface layer is highly anisotropic with an enhancement (reduction) parallel (perpendicular) to the walls. The effect of these anisotropic changes in the chain mobility near a free (or neutral) solid surface on the T_g value is not clear, and the situation is further complicated by the possibility of interactions between the polymer and solid surface. Experimentally, the T_g value that is measured for a given uncapped supported film seems to depend strongly on the details of the polymer-substrate interaction, as indicated by the different behavior measured for polymer films on different substrates [5]. In addition, the reductions in T_g observed by Keddie, Jones, and Cory reveal the importance of the free surface.

Because uncapped supported films have an inherently asymmetric film geometry with two different types of film interfaces (polymer-air and polymer-substrate), it is perhaps difficult to determine the effect of each interface on T_g by studying only uncapped supported films. To eliminate complications associated with the underlying substrate, we recently chose to eliminate the substrate and study freely-standing films. Using Brillouin light scattering (BLS) we measured T_g for a series of freely standing PS films (PS $M_w=767\times 10^3$; $R_{EE}=570$ Å) with film thicknesses 290 Å$<h<$1840 Å [3]. The T_g values were well described by the empirical relation

$$T_g(h)=\begin{cases} T_g^{\rm bulk}\left[1-\left(\dfrac{h_0-h}{\zeta}\right)\right], & h<h_0, \\ T_g^{\rm bulk}, & h\geqslant h_0. \end{cases} \tag{2}$$

As detailed in Ref. [3], we found that our data were much more consistent with Eq. (2) than with Eq. (1). The behavior described by Eq. (2) is as follows: for film thicknesses h greater than a threshold value h_0, the bulk T_g value is obtained, whereas for films with $h<h_0$, T_g decreases linearly with decreasing h. The best fit to the experimental data was obtained for $h_0=691\pm 20$ Å, and a slope parameter $\zeta=2130\pm 170$ Å. The linear dependence of T_g on h for $h<691$ Å is qualitatively different than the functional form of Eq. (1) used in Ref. [4] for uncapped PS films supported on Si. Although the measurements in Ref. [3] involved only a single value of $M_w=767\times 10^3$, the similarity between the h_0 value and $R_{EE}\sim 2R_g=570$ Å suggests a possible link between the T_g reductions and the confinement of the polymer chains.

In the present paper, we extend the BLS measurements on freely standing films to a second, larger M_w value ($M_w=2240\times 10^3$) to determine if the T_g reductions depend on the polymer chain length. We also use ellipsometry to study supported films of PS (of both M_w values) on SiO_x surfaces which are capped with a SiO_x layer. This choice of samples allows us to obtain direct T_g measurements on two different symmetric film geometries: freely standing films, with only polymer-air interfaces; and capped supported films, with

only polymer-SiO_x interfaces. In addition, we also present the results of T_g measurements of uncapped PS films supported on SiO_x surfaces, which have one polymer-air interface and one polymer-SiO_x interface. By measuring T_g for three different film geometries containing two different types of interfaces, we hoped to learn about the contribution of the two different interfaces to the overall measured T_g values for thin polymer films.

EXPERIMENT

Sample preparation

Polystyrene (PS), obtained from Polymer Source Inc., of two molecular weights was used: $\overline{M}_w = 767\times10^3$ ($\overline{M}_w/\overline{M}_n = 1.11$, $R_{EE} = 570$ Å) and $M_w = 2240\times10^3$ ($M_w/M_n = 1.08$, $R_{EE} = 970$ Å). The polymers were dissolved in toluene with PS concentrations (by mass) ranging from 0.8% to 3%.

Freely standing PS films were prepared by first spin coating the polymer solution onto a clean glass slide. The spin speed for the PS film deposition was 4000 rpm. The spin coated PS film was annealed at 100–130 °C for 12–20 h and then cooled at $\simeq$1 K/min through the glass transition temperature. After the film was annealed, it was cut into 1-cm^2 pieces and floated onto distilled water. A piece of the floating film was then transferred to a sample holder containing a small, 3-mm-diameter hole, creating a freely standing PS film. Other sections of the *same* floating film were transferred to Si wafers for film thickness measurements using ellipsometry. The freely standing PS film was heated slightly, to a temperature less than T_g, to remove residual water.

For the $\overline{M}_w = 767\times10^3$ PS molecules, seven freely standing films with thicknesses 290 Å$<h<$1840 Å were prepared. Six freely standing films of the higher $M_w = 2240\times10^3$ PS molecules were prepared with 586 Å$<h<$1800 Å. The sample details are given in Table I.

The preparation of uncapped and capped supported PS films required a more elaborate procedure. Since we wish to compare directly the T_g values obtained for all three sample geometries, the material for the underlying layer in both types of supported films and that for the capping layer material in the capped supported films must be the same. For the underlying and capping layer material we chose SiO_x, because it is a hard material which has little optical absorption and it can be evaporated directly onto the polymer films to produce sharp polymer-SiO_x interfaces [28]. Therefore, in all of the samples the PS film interfaces were either PS-air (free surface) or PS-SiO_x.

For the SiO_x layer evaporation, SiO powder was placed in a baffled tantalum boat (R. D. Mathis Co., model ME 1) and heated in vacuum to 70 °C for $\sim$12 h to remove adsorbed impurities. The ambient pressure in the evaporator was 1×10^{-6} torr, and the pressure during evaporation was $1-2\times10^{-5}$ torr. The SiO_x deposition rate was $\sim$1 Å/s as measured using a calibrated 5.0688-MHz crystal oscillator (M-Tron model MTO-T1-S3) and verified by performing ellipsometry on a series of SiO_x films of different thicknesses evaporated onto Si wafers. Ellipsometry measurements also allowed us to determine that the index of refraction of the SiO_x was consistent with $1<x<2$. The temperature of the films during evaporation, monitored using a copper-constantan thermocouple, was less than 70 °C for all films. Since this maximum temperature of the sample during evaporation was much lower than temperatures for which film dewetting has been observed, and since the samples were reannealed to 130 °C for 12–20 h after the entire sample preparation was completed, the modest temperature increases during evaporation were considered to be acceptable.

TABLE I. Film thicknesses h and glass transition temperature values T_g.

Film geometry	$\overline{M}_w = 767\times10^3$		$\overline{M}_w = 2240\times10^3$	
	h (Å)	T_g (K)	h (Å)	T_g (K)
Freely standing	290	303	586	310
	428	325	680	330
	540	336	700	354
	624	358	774	359
	632	360	1166	374
	830	368	1800	371
	1848	369		
Uncapped supported	290	361	390	366
	440	365	500	365
	660	366	624	366
	820	367	805	367
	1190	368	1200	367
			1720	370
Capped supported	290	359	390	361
	440	363	500	361
	660	364	624	366
	820	365	805	367
	1190	367	1200	370
	1840	367	1720	370

To prepare uncapped and capped supported PS films, a thin layer ($\sim$70 Å thick) of SiO_x was evaporated onto the bare Si wafer (with native oxide coating intact). For most samples the PS film was then spin coated directly onto the SiO_x layer. If the SiO_x-coated wafer exhibited any visible defect such as a dust particle, the PS layer was deposited onto the SiO_x-coated wafer using the water-transfer technique, since this produced a final sample of higher quality than those prepared by spin coating the PS layer directly onto the SiO_x-coated wafer with slight defects. For the $M_w = 767\times10^3$ PS molecules, five uncapped supported films with thicknesses 290 Å$<h<$1190 Å were prepared. Six uncapped supported films of the higher $M_w = 2240\times10^3$ PS molecules were prepared with 390 Å$<h<$1720 Å. The sample details are given in Table I.

To complete the preparation of the capped supported films, a thin layer ($\sim$70 Å thick) of SiO_x was evaporated onto the top PS film surface to produce samples with the configuration Si-SiO_x-PS-SiO_x. This ensured that the PS chain segments at both film surfaces had the same chemical environment. For samples containing very thin PS layers, we found that it was necessary to construct multilayers of

PS-SiO_x to obtain sufficient sample volume for the T_g measurements using ellipsometry. Because the optical absorption of the SiO_x layers was small, ellipsometry measurements of the multilayers were possible. Following the spin coating deposition of the first PS layer in the multilayer films, the deposition of subsequent PS layers using the water-transfer technique produced the highest-quality samples. Following the addition of each PS film, the sample was vacuum annealed at a temperature less than T_g (60–80 °C) for about 6 h. This modest annealing of the samples was performed to remove solvent and water without allowing the polymer chains to relax. Aggressive annealing at this stage could possibly lead to film dewetting. After the completion of the preparation of each capped supported sample, the sample was thoroughly annealed at 130 °C for 12–20 h. This final anneal allowed the polymer chains in each PS film to relax in the presence of both PS-SiO_x interfaces. The capping layer reduces the surface undulations which are necessary for film dewetting, and no evidence of dewetting was seen for any of the capped films after the final anneal. Every capped supported film was of sufficient quality to allow us to perform ellipsometry measurements since all samples contained areas free from defects that were much larger than the laser spot size ($\sim$1-mm diameter) in the ellipsometry experiment. For the sample areas chosen for the ellipsometry measurements, the amount of diffuse light scattering was indistinguishable from that for a clean Si wafer surface. The same polymer solutions used for spin coating the layers within the capped supported films were also used to make a series of uncapped films supported directly on Si wafers for film thickness measurements using ellipsometry.

For the $M_w = 767 \times 10^3$ PS molecules, six capped supported films with thicknesses 290 Å $< h <$ 1840 Å were prepared. Six capped supported films of the higher $M_w = 2240 \times 10^3$ PS molecules were prepared with 390 Å $< h <$ 1720 Å. The sample details are given in Table I.

Brillouin light scattering (BLS)

BLS has been used extensively to study the glass transition of both polymeric [29] and nonpolymeric [30] bulk materials. The scattering of light from thermally excited phonons travelling in the material allows the measurement of the frequency shift in the scattered light. The frequency shift measured in BLS experiments, which is typically several GHz, allows the determination of the velocity v of thermally excited, long wavelength ($\lambda_{ph} \sim 3000$ Å) phonons traveling in the material since $v = nf\lambda \sin(\theta/2)$, where n is the refractive index of the material, f is the measured frequency shift, λ is the light wavelength, and θ is the angle between the incident and scattered light. Typically light scattering from longitudinal phonons is observed, and the longitudinal sound velocity v_L is determined by material properties through the relation $v_L = \sqrt{c_{11}/\rho}$, where c_{11} is the longitudinal elastic constant and ρ is the material density. v_L is a strong function of ρ, since c_{11} has a strong nonlinear dependence on ρ, as revealed by BLS and ultrasonic studies of PS and other polymers at different pressures [31,33]. If v_L (or f) is measured as a function of temperature then, for temperatures $T < T_g$, the variation in the measured values with temperature is determined by the thermal expansivity of the glass, whereas, for $T > T_g$, the expansivity of the melt determines the observed behavior. Because of the discontinuity of the thermal expansivity at $T = T_g$, a sharp change or ''kink'' is observed at $T = T_g$ in the frequency versus temperature behavior that can be used to identify the glass transition temperature. It is important to note that BLS measurements of T_g using frequency versus temperature data give a measure of the temperature dependence of the density of the sample, and thus provide a low-frequency value of T_g despite the fact that the measured frequencies are in the GHz range. Relaxations at the measurement frequency are observed only at much higher temperatures [30,33].

For thin supported films a series of film-guided acoustic modes are observed [34]. These modes are dispersive with mode velocities which vary as the product $Q_\parallel h$, where $Q_\parallel$ is the phonon wave-vector component parallel to the film, and h is the film thickness. These modes are of mixed polarization being partially transverse and partially longitudinal in character. For BLS measurements of thin supported films, an optically absorbing substrate must be used since the large amount of light scattering from bulk phonons in transparent substrates would obscure the much weaker signal from the film-guided acoustic modes. Although BLS can be used to measure T_g for thin films supported on optically absorbing substrates [35], the focusing of the laser beam causes local heating in the substrate and therefore the film ($\sim$16 °C/100-mW laser power for a Si substrate and laser wavelength $\lambda = 5145$ Å) which complicates the determination of T_g.

For freely standing, optically transparent films BLS is an ideal tool for measuring T_g because the focussed laser beam produces no heating of the film, and the guided phonon mode velocities depend only on the film material. For freely standing films, the guided acoustic modes are referred to as Lamb modes [34] and are also of mixed polarization. The two lowest-velocity modes, however, are nearly purely polarized for small $Q_\parallel h$. The lowest-velocity mode (antisymmetric A_0) is primarily transverse in character, and its velocity approaches zero as $Q_\parallel h$ is decreased toward zero. The second-lowest-velocity mode (symmetric S_0) is essentially longitudinal for small $Q_\parallel h$, and it has the advantage that the mode velocity is only a weak function of $Q_\parallel h$ approaching a constant, nonzero value as $Q_\parallel h$ is decreased toward zero. This makes the S_0 mode ideal for comparisons to BLS studies of longitudinal phonons in bulk materials. We have recently shown that BLS is an effective tool to measure directly the T_g value for thin freely standing polymer films [3,36].

BLS studies were performed in air using the backscattering geometry, with the sample placed in an optical furnace [36] in which the sample temperature is controlled to within ± 0.25 K using a Eurotherm 808 temperature controller. Each spectrum is acquired with constant sample temperature, and the heating rate between fixed temperatures used for collecting consecutive BLS spectra is 0.5 K/min. Laser light (p polarized) with wavelength $\lambda = 5145$ Å is focused using a Nikon camera lens ($f/1.4$) onto the freely standing polymer film sample using an angle of incidence of $\theta_i = 45°$. The direction of the light reflected from the film is monitored visually to ensure that the value of θ_i, and therefore $Q_\parallel = (4\pi/\lambda)\sin\theta_i$, remains constant throughout the measurements. Backscattered ($\theta = 180°$) light is collected by the same camera lens used to focus the incident light. The col-

lected scattered light is focussed onto a 100-μm-diameter pinhole and recollimated. The collimated light passes through a narrow slit, which reduces the broadening of the Brillouin peaks produced by the nonzero light collection angle, and then is sent to a $3\times(1+1)$ tandem Fabry-Perot interferometer. Typical times required to obtain a BLS spectrum with acceptable signal-to-noise ratio for the S_0 peak (peak height to noise ratio ~ 40) are 5–50 min, depending on the film thickness and temperature.

Ellipsometry

Ellipsometry was first used in Ref. [37] to measure T_g of supported PS films. Keddie, Jones, and Cory [4,5] extended the technique to study a number of films with different values of film thickness h and molecular weight M_w.

For a transparent film supported on a substrate, measurements of the ellipsometric angles P (polarizer) and A (analyzer), or alternatively Δ and ψ, can be used to determine both the index of refraction n and film thickness h if the optical properties of the substrate are known [37]. If the angle of incidence is chosen properly, small changes in h in response to variations in, e.g., temperature lead to measurable changes in P and A. If data are acquired while heating or cooling the sample, the measured angles are simply linear functions of the sample temperature with a slope related to the thermal expansivity [5,37]. For supported films, the discontinuity of the expansivity at $T=T_g$ results in a ''kink'' in the ellipsometry angle versus temperature data which can be used to identify the T_g value [4,5,37]. For freely standing films the changes in P and A with h are so small that ellipsometry is not an effective technique for measuring T_g for such samples. Ellipsometry is, however, an ideal method for measuring T_g of both uncapped and capped supported polymer films. For very thin PS layers in the capped supported film geometry, small changes in the thickness of the PS layer with temperature were amplified by incorporating several identical polymer layers into a multilayered sample consisting of alternating layers of PS and SiO_x.

Ellipsometry measurements were performed using an EXACTA 2000 Faraday-modulated fast-nulling ellipsometer [38] in which a collimated, 1-mm-diameter He-Ne laser beam (light wavelength $\lambda = 6328$ Å) is directed onto the film surface. The sample was heated in air within a windowless, though almost fully enclosed, hot stage. The sample temperature was controlled to within ± 0.25 K using a Eurotherm 808 temperature controller. The sample temperature was first ramped at 10.0 K/min to 120–130 °C. The higher temperature was used for thicker polymer films. The sample temperature was maintained at this high value for 10–15 min, until the P and A values had stabilized. After this equilibration period the temperature was lowered at 1 K/min while recording the measured ellipsometric angles P and A on a computer. The P and A values were measured to within $\pm 0.003°$.

RESULTS AND DISCUSSION

Using the combination of BLS and ellipsometry techniques, the glass transition temperature T_g was measured for three different PS film geometries (freely standing, uncapped supported, and capped supported films) and two different values of M_w. This allows us to make comparisons between films with the same film geometries and different PS M_w values, as well as between films with different film geometries and the same PS M_w values.

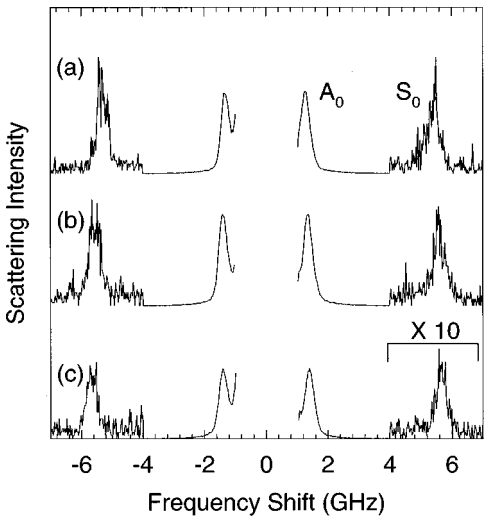

FIG. 1. BLS spectra for a freely standing PS film ($\overline{M_w} = 767 \times 10^3$) with thickness $h = 540$ Å for different temperatures: (a) 354.5 K, (b) 330.0 K, and (c) 303.5 K. For this film, $T_g = 336.0$ K. The two acoustic-phonon modes S_0 and A_0, which are labeled in (a), are observed in all spectra. For each spectrum, the laser power was 50 mW and the data collection time per channel was approximately 0.7 s.

Freely standing film data

A series of BLS spectra obtained for a freely standing PS film with thickness $h = 540$ Å for three different temperatures is shown in Fig. 1. Two acoustic-phonon modes are labeled in the figure. The lowest-frequency mode, the antisymmetric A_0 mode, has the largest light-scattering intensity in all spectra. However, because of its low frequency, the A_0 mode is obscured by the strong elastic peak (centered at 0 GHz), so that the mode is unsuitable for use in T_g measurements, particularly for films with thickness $h < 500$ Å. The symmetric S_0 mode, which occurs at higher frequencies, is ideal for T_g measurements since the mode frequency is insensitive to changes in h for $h < 1000$ Å and a fixed scattering geometry. For the thicker films, a higher-frequency antisymmetric A_1 mode was also observed. Since the frequency of this mode increases to very large values for small $Q_{\|}h$, it was not used to determine the value of T_g. The relative intensities of the different acoustic-phonon modes were observed to be strong functions of the film thickness. For some film thicknesses, light scattering from the S_0 mode was so intense that only 0.3-s total data collection time per channel of the multichannel scaler was sufficient to obtain an adequate signal-to-noise ratio (peak height to noise ratio ~ 40), whereas for other film thicknesses almost ten times as much data collection time was required to obtain comparable statistics. This high sensitivity of the acoustic-phonon mode intensities to film thickness also resulted in changes in the relative intensities of the modes for a single sample as the temperature was increased. Because of this effect, light scat-

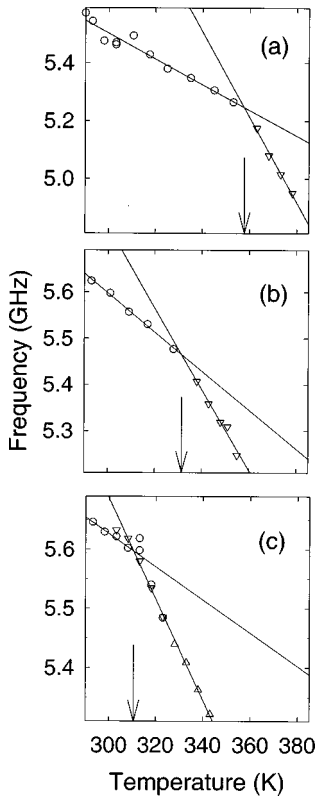

FIG. 2. Temperature dependence of the S_0 mode frequency for freely standing PS films ($M_w = 2240 \times 10^3$) of thicknesses (a) 774 Å, (b) 680 Å, and (c) 586 Å. The vertical arrows indicate the T_g values for each film. In (c), frequency values obtained on two different heating cycles are shown.

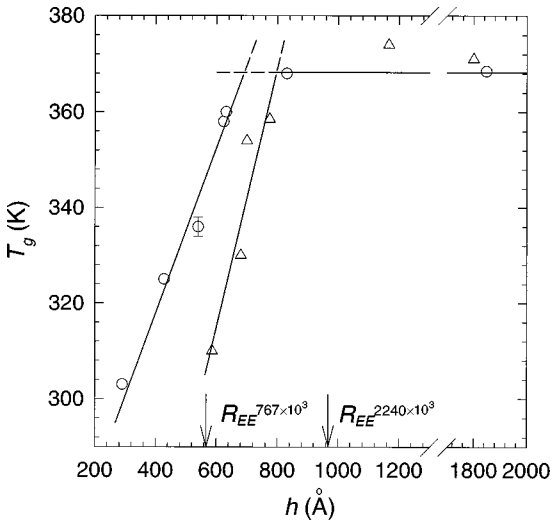

FIG. 3. T_g vs room-temperature film thickness h for freely standing PS films with $M_w = 767 \times 10^3$ (circles) and $M_w = 2240 \times 10^3$ (triangles). The straight lines were calculated using the best fit h_0 and ζ values [see Eq. (2)] for the data for each M_w value with $h < h_0$. The vertical arrows indicate the R_{EE} values for the two M_w values. An error bar which is representative of all of the data is shown for one of the data points.

tering from the S_0 mode decreased dramatically at elevated temperatures for some of the films, but this did not prevent the T_g measurement for these films.

To determine the value of T_g for a freely standing film, a series of BLS spectra were collected at fixed temperature values as the temperature was increased from room temperature. Typically 5–15 spectra were acquired for temperatures below T_g, and 4–6 spectra were acquired for temperatures greater than T_g. Fewer spectra were collected for temperatures $T > T_g$ because of the eventual formation of holes in the films at these temperatures. A nonlinear, least-squares fitting routine was used to obtain best fit values of the S_0 mode frequency immediately following the collection of each spectrum and before the temperature was increased for the collection of the next spectrum. This real-time tracking of the S_0 mode frequency allowed the use of smaller temperature steps once it was suspected that the temperature had been raised beyond T_g, as indicated by an increase in the slope of the S_0 mode frequency versus temperature plot. In Fig. 2 we show representative frequency versus temperature graphs that were used to determine the value of T_g for films made of the $M_w = 2240 \times 10^3$ polymer. A similar graph for the $M_w = 767 \times 10^3$ polymer has been published previously [3]. From Fig. 2 it is evident that, as in similar work on bulk glass-forming materials [30], the frequency versus temperature graph has two distinct linear regions. The two linear regions intersect at the glass transition temperature T_g. We estimate that the value of T_g can be determined to within ± 2 K using this method. In addition to this direct determination of T_g, during the BLS experiment there were indirect indications that T had been increased above T_g: fluctuations were observed in both the absolute intensity of the scattered light and the relative intensities of light scattering from the acoustic-phonon modes. For temperatures very near T_g (± 2 K) fluctuations in the intensity of the elastically scattered light sometimes made data collection difficult.

In Fig. 2(c), frequency values obtained on two different heating cycles are shown. The sample was cooled to room temperature at 0.5 K/min in between the two cycles. From the plot one can see that, except for the single data point for $T = T_g$, the measured frequencies are the same to within $\simeq 0.02$ GHz and, more importantly, the value of T_g is the same to within the quoted experimental accuracy of ± 2 K for both heating cycles. This reproducibility between successive heating cycles shows that there are no irreversible changes to the film when it is heated to temperatures slightly above T_g for time periods on the order of 1 h. This result provides evidence that helps to rule out film damage caused by reactions with atmospheric contaminants such as oxygen or water as a possible alternate cause for the large T_g reductions for freely standing PS films reported in Ref. [3] and the present paper.

In Fig. 3 are shown the measured T_g values as a function of room-temperature film thickness h for the freely standing PS films of both M_w values. The T_g values for the $M_w = 767 \times 10^3$ polymer, represented by circles in Fig. 3, are those published previously in Ref. [3] and are described by the empirical relation given by Eq. (2) with a threshold parameter value $h_0 = 691 \pm 20$ Å and a slope parameter value $\zeta = 2130 \pm 170$ Å. Qualitatively, the data obtained for the freely standing films of the $M_w = 2240$ k polymer, represented by triangles in Fig. 3, are the same as those obtained for the lower M_w polymer: the higher M_w data are also well

described by Eq. (2), with $h_0 = 796 \pm 25$ Å and $\zeta = 1360 \pm 200$ Å. As for the $M_w = 767 \times 10^3$ PS polymer [3], we note that the threshold value h_0 is close to $R_{EE} = 970$ Å for the $M_w = 2240 \times 10^3$ PS polymer. The straight lines shown in Fig. 3 were calculated using the best-fit h_0 and ζ values for the two M_w values. As for the lower M_w data, very large reductions in T_g are observed for the higher M_w data for film thicknesses less than the threshold parameter value h_0. However the data for films of the higher M_w polymer are shifted with respect to h. In particular, T_g reductions are observed for the higher M_w value at larger film thickness values than for the lower M_w value. This shift of the higher M_w data with respect to h is large, such that for film thicknesses h for which T_g reductions are observed for both molecular weights, e.g., $h = 600$ Å, the T_g value for the higher M_w is 40 K *lower* than for the lower M_w value.

This striking M_w dependence of the T_g reductions for freely standing PS films has two important implications. First of all, since large T_g reductions are obtained in freely standing films only for $h \lesssim R_{EE}$ for both M_w values, these results provide strong evidence that the large T_g reductions are directly related to the perturbation of the polymer molecules by confining them within films with thicknesses $h < R_{EE}$. Second, since a lower T_g value is obtained for the higher M_w value for a given film thickness, the large T_g reductions observed for freely standing films cannot be due to segregation of the chain ends at the surface of the films [18], since there is a smaller density of chain ends for the higher M_w polymer.

The large M_w dependence of the freely standing film data can also be used to address several concerns about our interpretation of our data. The most serious of these concerns is the possible effect of oxygen or water absorption at the PS-air interfaces. Although it is possible that surface reactions occur that change the chemical properties of the thinnest films, a difference of these reactions for two chemically identical polymers of different lengths is highly unlikely, and therefore this effect cannot be used to explain our data. Also, as the film thickness is reduced, in-plane stresses produced within the films due to the surface tension of PS in the freely standing film and the interfacial tension of PS and water during the water-transfer process may increase. However, these in-plane stresses will not depend on the M_w value of the polymer, so that this effect is also not consistent with our data. To assess the contribution of surface tension to the observed reductions in T_g, it is useful to calculate the magnitude of the associated in-plane stress. If the surface tension force is distributed uniformly across the thickness of the film for small h, the in-plane stress σ is given by $\sigma = 2\gamma/h$, where γ is the surface tension. For a PS film with thickness $h = 500$ Å, $\sigma = 1.6$ MPa. To estimate the effect of this in-plane stress on T_g, one can compare this value with hydrostatic pressure values needed to shift T_g: increasing the hydrostatic pressure of bulk PS by 100 MPa increases T_g by 28 K [31]. Therefore, the small in-plane tensile stress due to surface tension should reduce T_g by less than 1 K. This small shift in T_g due to the in-plane stress is likely an overestimate for the following reason. The shift in T_g for bulk hydrostatic pressures is due primarily to changes in density, whereas, for a freely standing PS film, the film will thin in response to in-plane stress, maintaining its density to be very close to its bulk value. Therefore the reduction in T_g for freely standing films due to surface tension should be less than that predicted on the basis of the hydrostatic measurements and much less than that observed in our experiments. If, instead of a uniform stress distribution across the thickness of the film, the surface tension is more localized at the film surfaces, e.g., within a few monomer lengths (~ 10 Å), the associated stresses will be correspondingly larger but one would not expect to observe the large T_g reductions for film thicknesses of several hundred Å which we measure in our experiments. Therefore, regardless of the stress distribution across the film thickness, surface tension does not explain our measured T_g values for freely standing films.

We note that there is not a simple relationship between h_0 and R_{EE} for the freely standing film data (see Fig. 3). In particular, for the $M_w = 767 \times 10^3$ polymer, $h_0 > R_{EE}$, and for the $M_w = 2240 \times 10^3$ polymer, $h_0 < R_{EE}$. However, it is true that the h_0 value increases with the size of the polymer molecules.

Comparison of freely standing film and supported film data

BLS can be used to measure T_g for very thin, transparent supported films; however, it is not ideal because of considerable heating of the film due to the absorption of the focused laser light by the underlying substrate. Instead, we used ellipsometry to measure the T_g values for uncapped and capped supported films. Because, in the ellipsometry experiment, the laser light is not focussed and the laser power is 50 times smaller than in the BLS experiment, there is no measurable heating produced by the laser light in the ellipsometry experiment.

Two representative samples of ellipsometry data for uncapped and capped supported films with $M_w = 2240 \times 10^3$ are shown in Fig. 4. As discussed in Refs. [4] and [37], for small changes in the film thickness both the polarizer (P) and analyzer (A) angles are linear functions of the film thickness in the glass and melt regimes. By performing linear fits to the P and/or A angles versus temperature data in the glass and melt regimes, a direct measure of T_g is obtained as the temperature corresponding to the intersection of the two straight lines. This method allowed us to determine T_g to within ± 1 K. Alternatively, calculation of the numerical derivative of the ellipsometry angles with respect to T can be used to determine T_g [5]; this resulted in T_g values that were within ± 1 K of those determined using the intersection of the two linear fits. It is worth noting that the data in Fig. 4 for the capped supported film were obtained from a multilayered sample consisting of two polymer layers, one which was spin coated and the other which was deposited using the water-transfer technique. The fact that such samples possess a single T_g value provides further evidence that the water-transfer procedure is not responsible for the large T_g changes reported previously for freely standing films [3]. For both values of M_w the ellipsometry data were accurately described by an isotropic film material with index $n = 1.59$.

In Fig. 5 we present the dependence of measured T_g values on room-temperature film thickness for the uncapped and capped supported films, together with the data for the freely standing films, for $M_w = 767 \times 10^3$. For film thicknesses $h < h_0 = 691$ Å, the T_g reductions are much larger for the

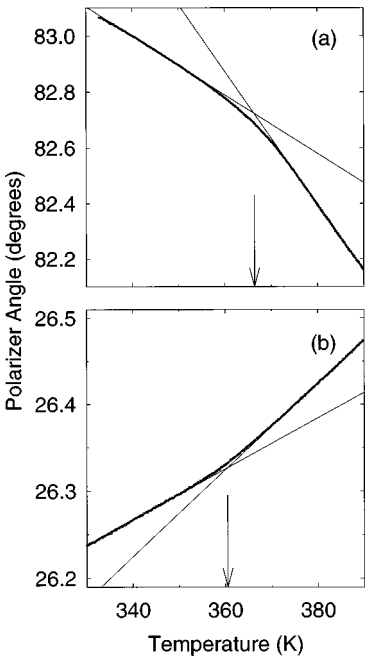

FIG. 4. Ellipsometry polarizer angle vs temperature for (a) a capped supported PS film consisting of two identical PS films ($M_w = 2240 \times 10^3$ and $h = 624$ Å) in a PS/SiO_x multilayer; and (b) an uncapped supported PS film ($M_w = 767 \times 10^3$ and $h = 290$ Å). The vertical arrows indicate the T_g values for each film.

freely standing films than for both the uncapped and capped supported films. Also, the data for the uncapped and capped supported films are quantitatively the same. In addition to our data, in Fig. 5 we also display two dashed lines which represent the spread and uncertainty in the results obtained in

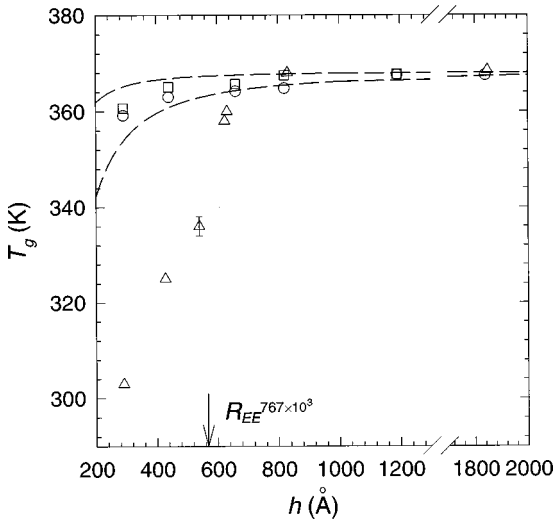

FIG. 5. T_g vs room-temperature film thickness h for all PS films with $M_w = 767 \times 10^3$. The data for freely standing, uncapped supported, and capped supported films are represented by triangles, squares, and circles, respectively. The dashed curves represent the spread and uncertainty of data for uncapped supported PS films on Si [4], which have been decreased by 5.6 K so that the T_g values obtained for thick films in Ref. [4] agree with those measured for the $M_w = 767 \times 10^3$ polymer. The vertical arrow indicates the R_{EE} value for the $M_w = 767 \times 10^3$ polymer.

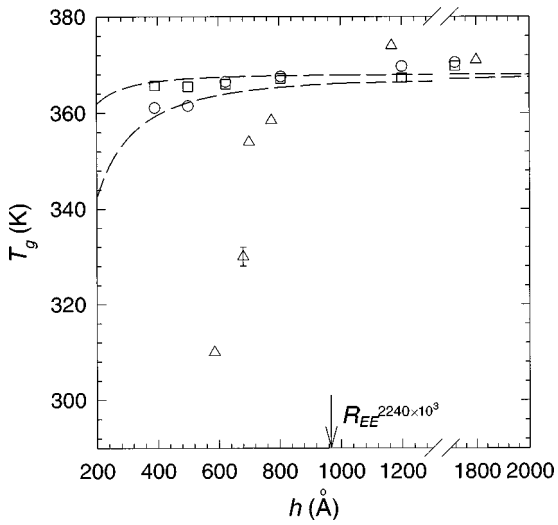

FIG. 6. T_g vs room-temperature film thickness h for all PS films with $M_w = 2240 \times 10^3$. The data for freely standing, uncapped supported, and capped supported films are represented by triangles, squares, and circles, respectively. The dashed curves represent the spread and uncertainty of data for uncapped supported PS films on Si [4], which have been decreased by 5.6 K so that the T_g values obtained for thick films in Ref. [4] agree with those measured for the $M_w = 767 \times 10^3$ polymer. The vertical arrow indicates the R_{EE} value for the $M_w = 2240 \times 10^3$ polymer.

Ref. [4] for uncapped supported PS films. Our data for uncapped supported films are consistent with Keddie, Jones, and Cory's previous ellipsometry measurements [4]. This similarity between the two sets of results provides some evidence that the films of Ref. [4] were on oxidized Si substrates, as proposed in Ref. [6].

In Fig. 6 we show the results of BLS and ellipsometry measurements of uncapped supported and capped supported PS films, together with the data for freely standing films, for $M_w = 2240 \times 10^3$. As for the results obtained for the lower M_w value, for film thicknesses $h < h_0 = 796$ Å the measured T_g values for the freely standing films are much lower than those measured for either the uncapped supported films or capped supported films. The measured T_g values for the uncapped supported films are again consistent with the results of Ref. [4], and those of the uncapped and capped supported films are essentially the same, except for the two thinnest films ($h = 390$ and 500 Å), for which the T_g values for the capped supported films are $\simeq 4$ K lower than those for the uncapped supported films. These small differences between the uncapped and capped supported film results are much smaller than those between the results for the freely standing films and either of the other film geometries.

We have investigated the possibility that the properties of the PS films were modified by the incident SiO_x particles during the evaporative deposition of the SiO_x capping layer. The deposition of SiO_x could affect the underlying PS film in two different ways. First, it is possible that the local heating produced by the hot SiO_x particles could cleave the PS chains which would reduce the M_w. Second, the implantation of SiO_x particles into the film could form defects in the film. This plasticizing effect [32] increases the local free volume which decreases T_g. We have addressed this issue of

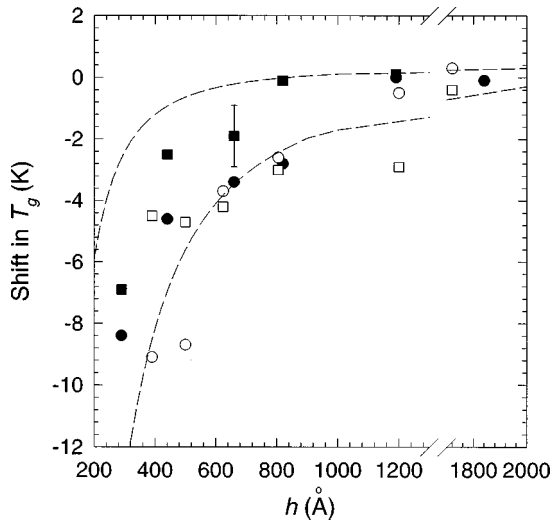

FIG. 7. Shift in T_g (relative to the bulk T_g value) vs room-temperature film thickness h for capped and uncapped supported PS films. Data are shown for $M_w = 767\times10^3$, uncapped (solid squares); $M_w = 767\times10^3$, capped (solid circles); $M_w = 2240\times10^3$, uncapped (open squares); and $M_w = 2240\times10^3$, capped (open circles). An error bar which is representative of all of the data is shown for one of the data points. The dashed curves represent the spread and uncertainty of data for uncapped supported PS films on Si [4].

possible PS film modification during the evaporation procedure by varying the SiO_x deposition rate, and therefore the temperature and flux of the SiO_x molecules. We prepared two identical uncapped PS films with $M_w = 767\times10^3$ and $h = 700$ Å. The films were then capped with SiO_x using deposition rates which differed by more than an order of magnitude (0.4 and 6 Å/s). The measured T_g values were the same to within 0.1 K for the two films. These results show that the PS films are not altered substantially during the SiO_x layer deposition.

Although one can see large differences between the measured T_g values for the freely standing films and those for the uncapped and capped supported films in Figs. 5 and 6, differences between the results obtained for uncapped and capped supported films for the two M_w values are not obvious. In Fig. 7 we plot the shift in T_g relative to the corresponding bulk T_g value versus the room-temperature film thickness for all of the supported films. As in Figs. 5 and 6, the dashed lines correspond to the spread and uncertainty in Keddie, Jones, and Cory's [4] data. The data are consistent with that of Keddie, Jones, and Cory. No evidence of a M_w dependence of the T_g values can be seen in our data for both types of supported films.

General discussion

To understand all of our data for freely standing, uncapped supported and capped supported films we propose the following explanation. The instantaneous shape of the constituent molecules in a polymer melt or a polymer glass is well described as ellipsoidal [24]. In a bulk sample, the ellipsoidal molecules are randomly oriented, and for many purposes can be thought of as spheres, which are characterized by an average value of the radius of gyration R_g. From computer simulations [21,22] it is known that, because of packing constraints, the effect of a hard neutral wall is to orient the major axis of the ellipsoidal molecules parallel to the wall, reducing the configurations of ellipsoids next to the wall. This loss of orientational entropy for molecules next to a hard neutral wall results in the radius of gyration perpendicular to the wall, $R_{g,\perp}$, smaller than that parallel to the wall, $R_{g,\parallel}$ (see, e.g., Ref. [39]). Also, for molecules next to a hard neutral wall, there is a corresponding enhancement of the chain mobility parallel to the wall which extends a distance approximately equal to R_{EE} from the wall [26,27].

The free surface of a polymer is a very good approximation to a hard neutral wall [40]. Near a free surface, the monomer density profile varies from zero to the bulk value over a distance which is very small compared with the size of the polymer molecule for high M_w values, corresponding to a sharp polymer-air interface. For freely standing films, which consist of polymer molecules confined between two free surfaces, we observe very large reductions in T_g for film thicknesses $h \lesssim R_{EE}$, which implies an increased segmental mobility of the molecules relative to that in bulk. Since these films consist only of molecules which are significantly perturbed by the presence of the free surfaces [26,27], our results provide experimental evidence that segmental mobility is increased by confining the polymer molecules with hard neutral walls in very thin polymer films.

An attractive interaction between the polymer chains and the hard wall will increase the number of contacts between the chains and the wall, decreasing the chain mobility and segmental motion of the molecules. For thin films the presence of an attractive interaction will produce smaller reductions in T_g relative to those for films with hard neutral walls, or perhaps even an increase in T_g for a strongly attractive polymer-wall interaction. In addition, because of the increased number of contacts between the polymer chains and the wall, the polymer-wall interaction will mask the M_w dependence of the results. Our results for PS films supported on SiO_x substrates, for which there is a weakly attractive interaction between the polymer and the substrate, as well as the results of other studies [4], are in agreement with this explanation. For the case of a strongly attractive polymer-substrate interaction an increase in T_g with decreasing film thickness h has been observed experimentally [7].

Because we measure essentially the same T_g values for uncapped supported films as we do for capped supported films, this suggests that the length scale of the polymer-substrate interaction is equal to or greater than R_{EE}. The results of lateral diffusion coefficient measurements for PS films on SiO_2 also suggest that the length scale of the polymer-substrate interaction is large [11,12].

In previous experiments on uncapped supported films described in the Introduction, it is interesting to note the relationship between the film thickness h and R_{EE}. Almost without exception, each T_g study involved films that were both thicker and thinner than R_{EE}. In contrast, almost all of the mobility experiments were performed only on films with thicknesses greater than R_{EE}. For some of the mobility studies [11], there was insufficient sensitivity in the experiment to probe thinner films. Given that we observe large reductions in T_g for freely standing films only for film thicknesses $h \lesssim R_{EE}$ and much smaller reductions in T_g for supported

films of comparable thicknesses, it is perhaps not surprising that increases in chain mobility are not observed for thicker supported films.

An examination of how our experimental results for freely standing films scale with the degree of polymerization N is perhaps unwarranted, since we have studied only two values of M_w. Notwithstanding this caveat, we can use the data that we obtained for freely standing films of two different M_w values to obtain approximate scaling laws for the two parameters of Eq. (2): $h_0 \sim N^{0.13\pm0.07}$ and $\zeta \sim N^{-0.42\pm0.11}$, where N is the degree of polymerization. The weak dependence of h_0 on N is an indication that there is not a simple relationship between h_0 and R_{EE}, as discussed above. It is interesting to note that the value h_0/ζ, which represents the reduction in T_g for a film of zero thickness [see Eq. (2)], scales as $h_0/\zeta \sim N^{0.55\pm0.13}$. Therefore, the scaling of h_0/ζ is essentially the same as that for the size of the polymer molecule R_{EE}. Measurement of freely standing films of additional M_w values will be necessary to determine if a detailed scaling analysis is warranted and, if so, to obtain accurate scaling laws.

SUMMARY AND CONCLUSIONS

We have measured the glass transition temperature T_g for polystyrene (PS) films as a function of film thickness h for two different PS molecular weight M_w values. Three different film geometries were studied: freely standing films, films supported on a SiO_x surface with the other film surface free (uncapped supported), and films supported on a SiO_x surface and covered with a SiO_x layer (capped supported). Large reductions in T_g were observed for the freely standing films: the measured T_g values decreased linearly with decreasing h for $h \lesssim R_{EE}$ (the average end-to-end distance of the unperturbed polymer molecules). This M_w dependence of the T_g reductions suggests that chain confinement effects are important. Smaller reductions in T_g were measured for both uncapped and capped supported films, with no significant dependence of the results on M_w and little difference between the results obtained for the two types of supported films. The similarity of the uncapped and capped supported film results suggests that the spatial extent of the polymer-substrate interaction is equal to or greater than R_{EE}.

ACKNOWLEDGMENTS

We thank Waterloo Digital Electronics for the use of their EXACTA 2000 ellipsometer. We thank Dr. B. G. Nickel for many insightful discussions. Financial support from NSERC of Canada is gratefully acknowledged.

[1] *Physics of Polymer Surfaces and Interfaces*, edited by I. C. Sanchez (Butterworth-Heinemann, Boston, 1992).
[2] *Polymers at Interfaces*, edited by G. J. Fleer, M. A. Cohen Stuart, J. M. H. M. Scheutjens, T. Cosgrove, and B. Vincent (Chapman and Hall, London, 1993).
[3] J. A. Forrest, K. Dalnoki-Veress, J. R. Stevens, and J. R. Dutcher, Phys. Rev. Lett. **77**, 2002 (1996).
[4] J. L. Keddie, R. A. L. Jones, and R. A. Cory, Europhys. Lett. **27**, 59 (1994).
[5] J. L. Keddie, R. A. L. Jones, and R. A. Cory, Faraday Discuss. Chem. Soc. **98**, 219 (1994).
[6] W. E. Wallace, J. H. van Zanten, and W. L. Wu, Phys. Rev. E **52**, R3329 (1995).
[7] J. H. van Zanten, W. E. Wallace, and W. L. Wu, Phys. Rev. E **53**, R2053 (1996).
[8] L. Xie, G. B. DeMaggio, W. E. Frieze, J. DeVries, D. W. Gidley, H. A. Hristov, and A. F. Yee, Phys. Rev. Lett. **74**, 4947 (1995).
[9] G. B. DeMaggio, W. E. Frieze, D. W. Gidley, M. Zhu, H. A. Hristov, and A. F. Yee, Phys. Rev. Lett. **78**, 1524 (1997).
[10] G. Reiter, Europhys. Lett. **23**, 579 (1993).
[11] B. Frank, A. P. Gast, T. P. Russell, H. R. Brown, and C. Hawker, Macromolecules **29**, 6531 (1996).
[12] X. Zheng, B. B. Sauer, J. G. Van Alsten, S. A. Schwartz, M. H. Rafailovich, J. Sokolov, and M. Rubinstein, Phys. Rev. Lett. **74**, 407 (1995).
[13] K. Tanaka, A. Taura, S.-R. Ge, A. Takahara, and T. Kajiyama, Macromolecules **29**, 3040 (1996); T. Kajiyama, K. Tanaka, and A. Takahara, *ibid.* **30**, 280 (1997).
[14] M. F. Toney, T. P. Russell, J. A. Logan, H. Kikuchi, J. M. Sands, and S. K. Kumar, Nature (London) **374**, 709 (1995).
[15] M. G. Samant, J. Stöhr, H. R. Brown, T. P. Russell, J. M. Sands, and S. K. Kumar, Macromolecules **29**, 8334 (1996).
[16] Y. Liu, T. P. Russell, M. G. Samant, J. Stöhr, H. R. Brown, A. Cossy-Favre, and J. Diaz (unpublished).
[17] D. B. Hall, J. C. Hooker, and J. M. Torkelson, Macromolecules **30**, 667 (1997).
[18] A. M. Mayes, Macromolecules **27**, 3114 (1994).
[19] P.-G. de Gennes, C. R. Acad. Sci. (Paris) **307**, 1841 (1988).
[20] W. Zhao, X. Zhao, M. H. Rafailovich, J. Sokolov, R. J. Composto, J. J. Smith, W. D. Dozier, J. Mansfield, and T. P. Russell, Macromolecules **26**, 561 (1993).
[21] J. Baschnagel and K. Binder, Macromolecules **28**, 6808 (1995).
[22] T. Pakula, J. Chem. Phys. **95**, 4685 (1991).
[23] G. ten Brinke, D. Ausserre, and G. Hadziioannou, J. Chem. Phys. **89**, 4374 (1988).
[24] See, e.g., J. Mazur, C. M. Guttman, and F. L. McCrackin, Macromolecules **6**, 872 (1973).
[25] K. F. Mansfield and D. N. Theodorou, Macromolecules **23**, 4430 (1990).
[26] K. F. Mansfield and D. N. Theodorou, Macromolecules **24**, 6283 (1991).
[27] J. Baschnagel and K. Binder, J. Phys. I **6**, 1271 (1996).
[28] P. Lambooy, J. R. Salem, and T. P. Russell, Thin Solid Films **252**, 75 (1994).
[29] R. W. Coakley, R. S. Mitchell, J. R. Stevens, and J. L. Hunt, J. Appl. Phys. **47**, 4271 (1976).
[30] J. E. Masnik, J. Kieffer, and J. D. Bass, J. Chem. Phys. **103**, 9907 (1995).

[31] J. R. Stevens, R. W. Coakley, K. W. Chau, and J. L. Hunt, J. Chem. Phys. **84**, 1006 (1986).

[32] See, e.g., J. M. G. Cowie, *Polymers: Chemistry and Physics of Modern Materials*, 2nd ed. (Chapman and Hall, New York, 1991).

[33] A. Sahnoone, F. Massines, and L. Piche, in *Disordered Materials and Interfaces*, edited by H. G. Stanley, H. Z. Cummins, D. J. Dorian, and D. L. Johnson, MRS Symposia Proceedings No. 407 (Materials Research Society, Pittsburgh, 1995).

[34] G. W. Farnell and E. L. Adler, in *Physical Acoustics, Principles and Methods*, edited by W. P. Mason and R. N. Thurston (Academic, New York, 1972), Vol. 9, Chap. 2.

[35] J. R. Dutcher and K. Dalnoki-Veress (unpublished).

[36] J. A. Forrest, K. Dalnoki-Veress, J. R. Stevens, and J. R. Dutcher, in *Disordered Materials and Interfaces* (Ref. [33]), p.131.

[37] G. Beaucage, R. J. Composto, and R. S. Stein, J. Polym. Sci. Polym. Phys. Ed. **30**, 131 (1993).

[38] Waterloo Digital Electronics, Waterloo, Ontario, Canada N2J 3H8.

[39] H. R. Brown and T. P. Russell, Macromolecules **29**, 798 (1996).

[40] D. T. Wu, G. H. Fredrickson, J.-P. Carton, A. Ajdari, and L. Leibler, J. Polym. Sci. Polym. Phys. **33**, 2373 (1995).